

Accelerator R&D at Fermilab's FAST/IOTA for Future High Intensity Proton Accelerators

B. Freemire* for the FAST/IOTA Team

Northern Illinois University, DeKalb, Illinois 60115, USA

E-mail: bfreemire@niu.edu

The physics programs of future hadron accelerators require larger beam current and power than existing facilities can provide. New facilities are being designed and existing accelerators upgraded in order to meet this demand. A significant impediment for such high intensity accelerators is beam loss, which both damages and activates accelerator components. Losses must therefore be minimized, and the Fermilab Accelerator Science and Technology (FAST) facility team is building a storage ring, the Integrable Optics Test Accelerator (IOTA), to investigate accelerator technology for the next generation of particle accelerators. IOTA will host a variety of experiments with the goal of better understanding and controlling space charge effects and incoherent instabilities, while developing techniques to minimize beam loss.

The 19th International Workshop on Neutrinos from Accelerators-NUFACT2017

25-30 September, 2017

Uppsala University, Uppsala, Sweden

*Speaker.

1. Introduction

Currently, there are only two accelerators in the world operating at 1 MW or above: the Spallation Neutron Source (SNS) at Oak Ridge National Laboratory, and the High Intensity Proton Accelerator (HIPA) at the Paul Scherrer Institut. Plans exist for upgrading or building a number of accelerators to operate above 1 MW proton beam power, of which notable examples include the Japan Proton Accelerator Research Complex (J-PARC) [1], the European Spallation Source (ESS) [2], and Fermi National Accelerator Laboratory (Fermilab) [3].

A major impediment in achieving beam power above 1 MW is controlling losses, which lead to damage and activation of accelerator components. At high beam intensity, these losses are primarily due to space charge. J-PARC recently demonstrated 1 MW beam operation with beam loss on the order of 10^{-3} [1], with routine operation at 1 MW expected to begin soon. The upgrade plans for Fermilab's accelerator complex involve a series of improvements, beginning with operation at 700 kW with 120 GeV protons, before moving to 1.2 MW, and finally reaching >2 MW beam power to satisfy the Deep Underground Neutrino Experiment's (DUNE) experimental program.

Fermilab's Proton Improvement Plan II (PIP-II) is expected to deliver 1.2 MW beam power [4]. PIP-II will accomplish this by replacing the existing 400 MeV normal conducting linac with an 800 MeV superconducting linac capable of continuous wave operation. This will allow a 50% increase in beam intensity in the following accelerator sections, along with a 30% decrease in the space charge tune shift. Additional upgrades to the accelerator complex are also required in order to accelerate 50% more beam, including increasing the repetition rate in the Booster from 15 to 20 Hz.

In order to achieve the 2.5 MW goal of DUNE/LBNF, upgrades to the Fermilab accelerator complex beyond PIP-II are required. The so-called PIP-III currently consists of replacing the existing Booster with one of two options: an 8 GeV superconducting linac, or a rapid cycling synchrotron (RCS) [5]. Recent breakthroughs in nitrogen processing of SRF cavities have produced encouraging results for the former option (see, e.g. [6]). An experimental facility is being built and commissioned at Fermilab in an effort to pursue the latter option. The techniques that will be tested there are being applied to an "integrable" RCS design (see, e.g. [7]).

The following sections outline the facility and experimental program in place at Fermilab aimed at achieving cost effective multi-MW beams.

2. Fermilab Accelerator Science and Technology Facility & Integrable Optics Test Accelerator

The Fermilab Accelerator Science and Technology (FAST) facility aims to support research and development of accelerator technology for the next generation of particle accelerators. FAST is home to a 150 MeV/c electron beam derived from a photoinjector based superconducting radio frequency (SRF) linear accelerator, and will also house a 68.5 MeV/c proton beam derived from a low duty factor radio frequency quadrupole (RFQ). Recently, the electron linac was commissioned up to 300 MeV total beam energy, with 250 MeV energy gain in the SRF cryomodule. Figure 1 shows the electron linac, proton RFQ source, and both beam transport lines into the IOTA storage ring.

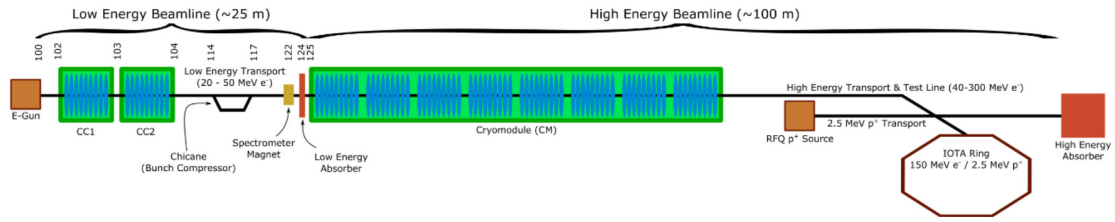


Figure 1: Schematic of the electron and proton beamlines at FAST (not to scale).

Construction is underway on the main experimental platform at FAST, the Integrable Optics Test Accelerator (IOTA). IOTA is a storage ring that will accept either the electron or proton beam from FAST. Its purpose is to investigate techniques for producing higher brightness beams for the next generation of high intensity proton facilities. Figure 2 shows a three dimensional schematic of IOTA, as well as the magnet configuration for the ring. Table 1 lists the parameters for IOTA for electrons and protons.

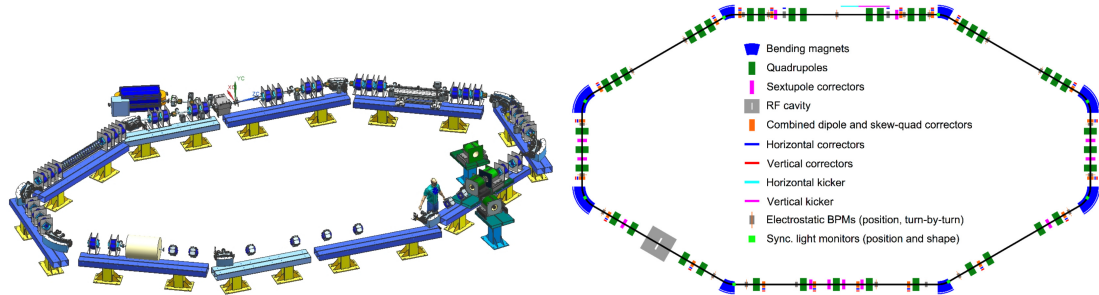


Figure 2: 3D model of IOTA (left). 2D model of IOTA showing the locations of the magnets, as well as the RF cavity and some beam instrumentation (right). Beam will be injected at the long straight section at the top. The nonlinear magnets will be placed in the experimental straight sections at the top corners. The electron lens/column will be in the straight section at the bottom right, while the optical stochastic cooling experiment will be in the straight section at the bottom in the center.

3. IOTA Experimental Program

The goal of IOTA is to pursue techniques aimed at understanding and controlling proton beam instabilities, losses, and halo formation. A number of the planned experiments are outlined below. See Ref. [8] for a more complete list. The lattice of IOTA is tunable to accommodate the host of experiments.

3.1 Nonlinear Integrable Optics

Accelerators are based on linear focusing elements (dipole and quadrupole magnets), but require nonlinear focusing elements (sextupole and octupole, etc.) in order to correct for chromaticity and allow for Landau damping. These nonlinear elements push the system far from integrable, which limits the nonchaotic phase space of the beam. Should the system be integrable initially, chaotic volume regions are minimized, even for off-momentum particles.

Parameter	e Value	p Value	Units
Ring circumference	40		m
Experimental straight sections	4		
Nominal bending field	0.7		T
Vacuum	$\leq 3 \times 10^{-8}$	$\leq 6 \times 10^{-10}$	torr
RF cavity frequency	30	2.18	MHz
Momentum (Kinetic Energy)	150 (150)	68.5 (2.5)	MeV/c (MeV)
Revolution period	0.133	1.83	μ s
Number of particles (beam current)	2×10^9 (2.4)	9×10^{10} (8)	(mA)
Equilibrium transverse emittance	0.04	0.3	μ m
Synchrotron tune	5.3×10^{-4}	7×10^{-3}	
Beam energy spread	1.35×10^{-4}	1.5×10^{-3}	
Bunch length	0.0108	1.7	m
Maximum space charge parameter (ΔQ_{SC})	~ 0	≥ 0.5	

Table 1: IOTA beam parameters [8].

A number of nonlinear integrable accelerator lattices have been proposed to produce regular particle orbits in a large phase space around the reference particle [9]. One such lattice will be implemented in IOTA. The element of lattice periodicity will be comprised of a drift space with equal beta functions, followed by an optics insert, made of linear elements, that has the transfer matrix of a thin axially symmetric lens. If an additional transverse magnetic field is applied along the drift space, the system has two integrals of motion. The betatron phase advance over the drift space is limited to 0.5, while the phase advance in the optics insert must be a multiple of 0.5 (all in units of 2π). This gives the maximum full tune for one element of periodicity of $0.5 + 0.5 \times n$ (n is an integer), and in terms of the full betatron tune per cell, the tune shift can reach 50%.

The Hamiltonian describing a particle moving through a drift space with an additional potential is

$$H = \frac{p_x^2 + p_y^2}{2} + \frac{x^2 + y^2}{2} + \beta(\psi) V(x\sqrt{\beta(\psi)}, y\sqrt{\beta(\psi)}, s(\psi)) \quad (3.1)$$

where $\psi' = 1/\beta(s)$. The potential must be time-independent to produce the first integral of motion, i.e.

$$\beta(\psi) V(x\sqrt{\beta(\psi)}, y\sqrt{\beta(\psi)}, s(\psi)) = \frac{x^2 + y^2}{2} + t \frac{\xi \sqrt{\xi^2 - 1} \cosh^{-1}(\xi) + \eta \sqrt{\eta^2 - 1} (\frac{\pi}{2} + \cosh^{-1}(\eta))}{\xi^2 - \eta^2} \quad (3.2)$$

with

$$\xi = \frac{\sqrt{(x+c)^2 + y^2} + \sqrt{(x-c)^2 + y^2}}{2c}, \quad \eta = \frac{\sqrt{(x+c)^2 + y^2} - \sqrt{(x-c)^2 + y^2}}{2c} \quad (3.3)$$

where t is the magnet strength parameter, and c is the geometric parameter that represents the distance between singularities (pole tips). The potential must continuously change along the nonlinear insert, which is approximated by 18 thin magnets of constant aperture. The length of the nonlinear

insert is 1.8 m and the betatron phase advance in the drift is 0.3, corresponding to a minimum beta function of 0.6 m and a maximum of 2 m. The geometric parameter, c , varies accordingly from 8 to 14 mm, meaning the horizontal beam pipe aperture is between 12 and 21 mm. IOTA has been designed to accommodate one and two nonlinear magnet inserts. The beta and dispersion functions for the case of a single nonlinear magnet is shown in Fig. 3.

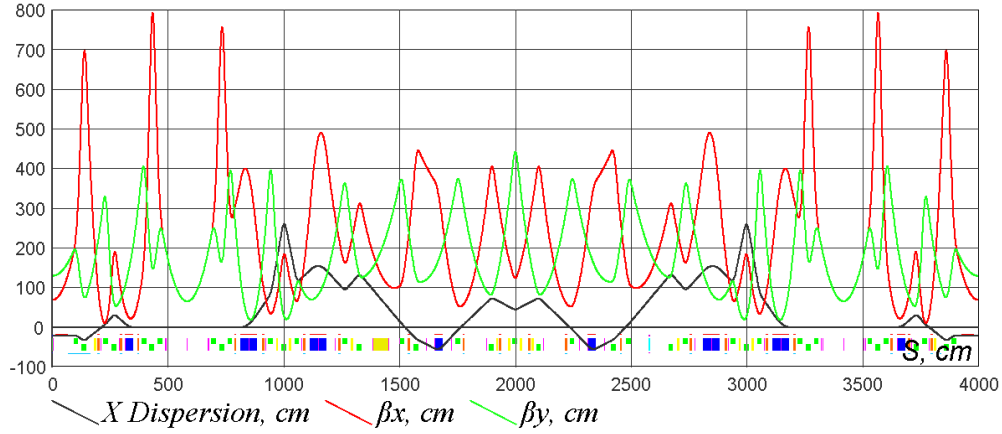


Figure 3: Beta and dispersion functions for the IOTA lattice with one nonlinear magnet [10]. Injection is at $s=0$, while the nonlinear magnets can be placed at $s=600$ and 3400 cm.

Initial experiments with an electron beam will demonstrate a large nonlinear amplitude-dependent tune shift without reduction of the dynamical aperture. Experiments with a proton beam will be used to study the conservation of the invariants and integrability in the presence of space charge.

3.2 Electron Lenses

Electron lenses are used to actively manipulate circulating beams by injecting a pulsed, magnetically confined electron beam co-propagating with the main beam [11]. In IOTA, an electron lens will be used as a nonlinear element to provide a tunable transverse kick to the beam dependent on its betatron amplitude [12]. The focusing strength of the lens acting on a circulating beam with small betatron amplitudes is

$$k_e = 2\pi \frac{j_0 L (1 \pm \beta_e \beta_z)}{B\rho \beta_e \beta_z c^2} \left(\frac{1}{4\pi \epsilon_0} \right) \quad (3.4)$$

where j_0 is the on-axis electron current density, L is the length of the lens, $\beta_{e,z}$ is the relativistic factor for electrons and the beam, and $B\rho$ is the magnetic rigidity. The corresponding tune shift for small strengths and away from half-integer resonances is

$$\Delta \nu = \frac{\beta k_e}{4\pi} = \frac{\beta j_0 L (1 \pm \beta_e \beta_z)}{2B\rho \beta_e \beta_z c^2} \left(\frac{1}{4\pi \epsilon_0} \right) \quad (3.5)$$

where β is the transverse betatron amplitude. Two types of electron lenses will be tested in IOTA: a thin McMillan type, and a thick axially symmetric type.

The thin McMillan type provides a nonlinear transverse kick as a function of amplitude. It depends on creating and preserving a current density of the form

$$j(r) = \frac{j_0 a^4}{(r^2 + a^2)^2} \quad (3.6)$$

The beam experiences a nonlinear transverse kick

$$\theta(r) = \frac{k_e a^2 r}{r^2 + a^2} \quad (3.7)$$

If the betatron phase advance in the rest of the ring is near an odd multiple of $\pi/2$ and the lens is sufficiently thin, there are two invariants of motion in the 4D transverse phase space, resulting in regular and bounded trajectories (neglecting longitudinal effects). The achievable tune spread is dependent on the transverse beta functions and the focusing strength of the lens (as in Eq. 3.5).

For the axially symmetric thick lens, the beta functions must be constant and equal over the length of the lens. This can be accomplished with a solenoid with an axial field of the form $B_z = 2B\rho/\beta$, which also confines the electrons in the lens. For a betatron phase advance in the rest of the ring that is an integer multiple of π , the Hamiltonian and longitudinal component of angular momentum are conserved. The achievable tune spread in this case is proportional to $L/2\pi\beta$, because the machine operates near integer or half-integer resonances.

The thin McMillan lens allows for a larger tune spread, but is dependent on the shape of the electron current distribution, while the thick axially symmetric lens is more robust (being independent of current distribution), however allows a smaller tune spread. An electron lens will be created using an electron gun, then confining and transporting the electron beam using strong axial magnetic fields to an interaction region in which it overlaps with the beam, before being steered into a collector. Figure 4 shows a schematic of the electron lens in IOTA.

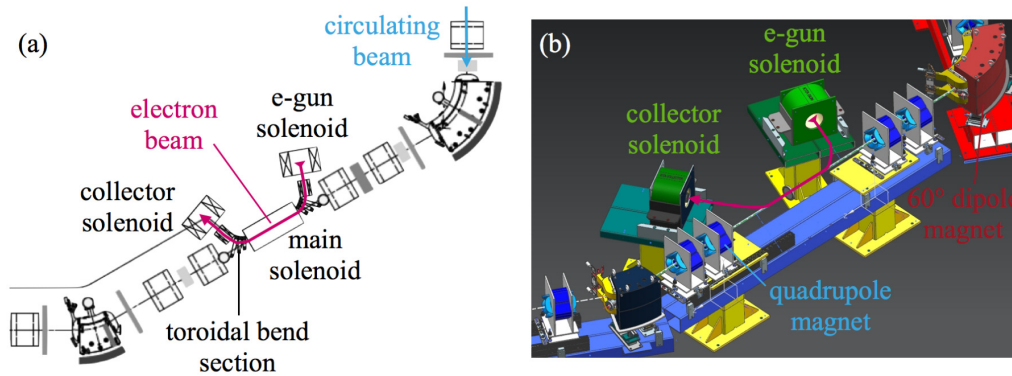


Figure 4: Schematic of the electron lens in IOTA [8].

3.3 Space Charge Compensation

Space charge is frequently the limiting factor in accelerating high current beams. The space charge force leads to emittance growth and instabilities, and ultimately beam loss. A number of techniques have been employed to compensate space charge, however a practical method of neutralizing space charge in a ring has not been demonstrated.

In IOTA, two methods of space charge compensation will be investigated. Both neutralize the space charge force by creating an electron distribution that matches that of the circulating proton beam. The first method is similar to the electron lens in that it works by using an electron gun to generate the desired distribution, then injecting the electrons into the ring, co-propagating with the proton beam [13]. After a short distance, the electrons are extracted from the ring (see Fig. 4). The second method does not rely on an external source of electrons, but rather utilizes the plasma electrons generated by the beam ionizing a short section of gas [14]. The plasma electrons are shaped to the appropriate distribution using electric and magnetic fields. Figure 5 shows the setup for the electron column.

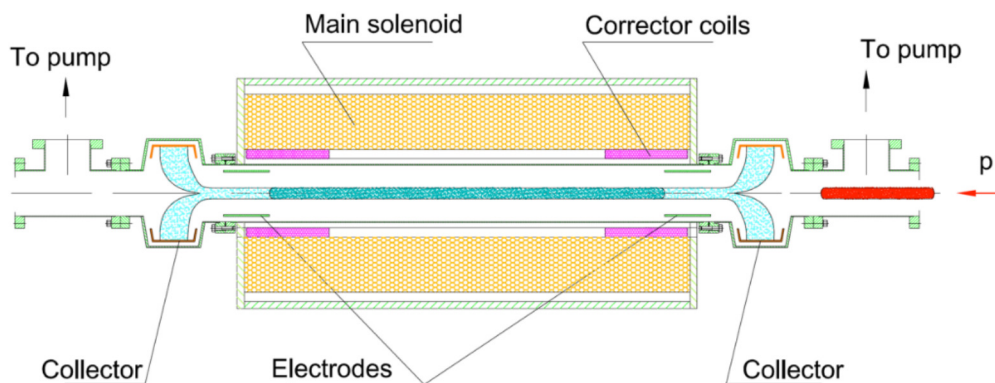


Figure 5: Schematic of the electron column in IOTA [8]. The proton beam enters from the right and traverses a region of relatively high gas density, bounded by the collectors, in which the electron distribution is matched.

4. Outlook

The electron beamline of FAST has recently been commissioned to an energy of 300 MeV, exceeding the injection energy of electrons into IOTA (150 MeV), while reaching the design accelerating gradient of 31.5 MV/m for the SRF cryomodule. An experimental run that included higher order mode studies of the RF cavities, round to flat beam transformation efforts, and short electron bunches produced by a z-slicer was successfully completed. FAST has begun a shutdown during which time installation of IOTA will be completed. The first electrons are expected to be injected into IOTA during the summer of 2018. Following an experimental run with electrons, FAST will have another shutdown in order to install the proton RFQ and beamline. It is expected to have protons in IOTA during 2019-2020.

5. Acknowledgements

The author would like to thank the FAST/IOTA team, in particular V. Shiltsev, A. Valishev, S. Nagaitsev, G. Stancari, and E. Prebys, for contributing to these proceedings. This work is supported by the U.S. Department of Energy Office of Science under Contract No. DE-AC02-07CH11359 and the US Department of Energy Office of High Energy Physics General Accelerator Research and Development (GARD) Program.

References

- [1] H. Hotchi, et.al., *Achievement of a low-loss 1-MW beam operation in the 3-GeV rapid cycling synchrotron of the Japan Proton Accelerator Research Complex*, Phys. Rev. Accel. Beams, **20**, 6, 060402 (2017).
- [2] S. Peggs, et.al., *ESS Technical Design Report*, ver. 3.08, (2017).
- [3] V. Shiltsev, *Fermilab Proton Accelerator Complex Status and Improvement Plans*, Mod. Phys. Lett. A, **32**, 16, 1730012 (2017).
- [4] I. Kourbanis, *FNAL Accelerator Complex Upgrade Possibilities*, in *Proceedings of NAPAC'16*, THA3IO01, Chicago, USA, Oct. 2016.
- [5] V. Shiltsev, *Fermilab Accelerator R&D Program Towards Intensity Frontier Accelerators: Status and Progress*, in *Proceedings of NAPAC'16*, WEPOA25, Chicago, USA, Oct. 2016.
- [6] M. Martinello, et.al., *Surface Impurity Content Optimization to Maximize Q-Factors of Superconducting Resonators*, in *Proceedings of NAPAC'16*, WEB1CO03, Chicago, USA, Oct. 2016.
- [7] J. Eldred and A. Valishev, *Design Considerations for Proposed Fermilab Integrable RCS*, in *Proceedings of NAPAC'16*, THPOA19, Chicago, USA, Oct. 2016.
- [8] S. Antipov, et.al., *IOTA (Integrable Optics Test Accelerator): facility and experimental beam physics program*, Journal of Instrumentation, **12**, 03, (2017).
- [9] V. Danilov and S. Nagaitsev, *Nonlinear Accelerator Lattices with One and Two Analytic Invariants*, Phys. Rev. ST Accel. Beams, **13**, 084002 (2010).
- [10] A. Romanov, *IOTA Optics Update: Flexibility for Experiments*, FAST/IOTA Collaboration Meeting, June 6, 2017.
- [11] V. Shiltsev, et.al., *Experimental Demonstration of Compensation of Beam-Beam Effects by Electron Lenses*, Phys. Rev. Lett., **99**, 244801 (2007).
- [12] G. Stancari, et.al., *Electron Lenses and Cooling for the Fermilab Integrable Optics Test Accelerator*, in *Proceedings of COOL'15*, MOPF03, Newport News, USA, Sept. 2015.
- [13] A.V. Burov, G.W. Foster and V.D. Shiltsev, *Space-Charge Compensation in High-Intensity Proton Rings*, FERMILAB-TM-2125 (2000).
- [14] V. Shiltsev, et.al., *The Use of Ionization Electron Columns for Space-Charge Compensation in High Intensity Proton Accelerators*, AIP Conf. Proc., **1086**, 649, (2009).